Lab on a Chip

PAPER

View Article Online
View Journal | View Issue

Cite this: *Lab Chip*, 2015, **15**, 745

Measuring direct current trans-epithelial electrical resistance in organ-on-a-chip microsystems†

Mathieu Odijk,*[a] Andries D. van der Meer,[b] Daniel Levner,[b] Hyun Jung Kim,[b] Marinke W. van der Helm,[a] Loes I. Segerink,[a] Jean-Phillipe Frimat,[a] Geraldine A. Hamilton,[b] Donald E. Ingber[b] and Albert van den Berg[a]

Trans-epithelial electrical resistance (TEER) measurements are widely used as real-time, non-destructive, and label-free measurements of epithelial and endothelial barrier function. TEER measurements are ideal for characterizing tissue barrier function in organs-on-chip studies for drug testing and investigation of human disease models; however, published reports using this technique have reported highly conflicting results even with identical cell lines and experimental setups. The differences are even more dramatic when comparing measurements in conventional Transwell systems with those obtained in microfluidic systems. Our goal in this work was therefore to enhance the fidelity of TEER measurements in microfluidic organs-on-chips, specifically using direct current (DC) measurements of TEER, as this is the most widely used method reported in the literature. Here we present a mathematical model that accounts for differences measured in TEER between microfluidic chips and Transwell systems, which arise from differences in device geometry. The model is validated by comparing TEER measurements obtained in a microfluidic gut-on-a-chip device *versus* in a Transwell culture system. Moreover, we show that even small gaps in cell coverage (*e.g.*, 0.4%) are sufficient to cause a significant (~80%) drop in TEER. Importantly, these findings demonstrate that TEER measurements obtained in microfluidic systems, such as organs-on-chips, require special consideration, specifically when results are to be compared with measurements obtained from Transwell systems.

Received 14th October 2014,
Accepted 18th November 2014

DOI: 10.1039/c4lc01219d

www.rsc.org/loc

Introduction

Trans-epithelial electrical resistance (TEER) is a widely used parameter to characterize the quality of the barrier function of epithelial and endothelial cell monolayers. In principle, measuring TEER across the barrier is a non-destructive, label-free method, providing real-time information on barrier quality. Therefore, it is an ideal and relatively low-cost method to monitor cell growth in organ-on-a-chip microfluidic systems.[1] The aim of this article is to consider issues that arise when TEER is measured in microfluidic systems, particularly when the results of these measurements are compared with values found in conventional monolayer or bi-layer culture systems, such as Transwell culture devices.

A schematic model of a typical tissue barrier consisting of a culture of epithelial or endothelial cells is shown in Fig. 1. In principle, two pathways exist for ion transport across the cell monolayer: 1) the transcellular pathway, which includes lipophilic, receptor-mediated, adsorptive and protein transport, and 2) the paracellular route that involves transport through cell junctions and the intercellular space.[2]

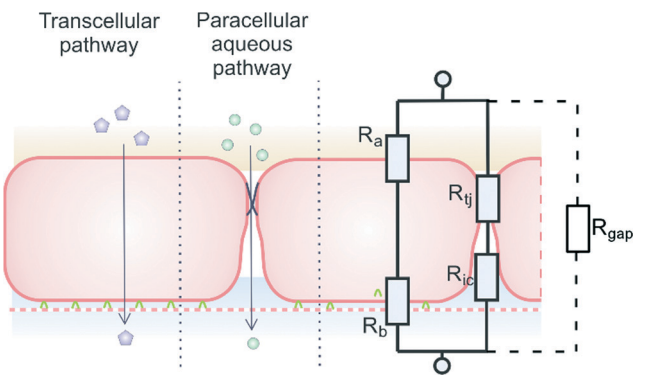

Fig. 1 Endothelial cell layer forming a barrier, image based on Abbott *et al.*[2] The extra gap resistance (R_{gap}) pathway is discussed in more detail in the next sections.

[a] *BIOS/Lab-on-Chip Group, MESA+ Institute for Nanotechnology & MIRA Institute for Biomedical Technology and Technical Medicine, University of Twente, P. O. Box 217, 7500 AE Enschede, The Netherlands. E-mail: m.odijk@utwente.nl; Fax: +31 534893595; Tel: +31 534894782*

[b] *Wyss Institute for Biologically Inspired Engineering at Harvard University, CLSB Bldg. 5th floor, 3 Blackfan Circle, Boston, MA 02115, USA. E-mail: don.ingber@wyss.harvard.edu; Fax: +1 617 432 7048; Tel: +1 617 432 7044*

† Electronic supplementary information (ESI) available. See DOI: 10.1039/c4lc01219d

A relatively simple equivalent circuit model can be made for this barrier, as shown in Fig. 1 in which the transported ions and other charged molecules are the charge carriers in the system. The transcellular pathway R_{trc}, is the sum of the apical cell membrane resistance (R_a) and the basolateral cell membrane resistance (R_b). R_{pc} depicts the paracellular pathway and is equal to the sum of the tight junction resistance (R_{tj}) and the intercellular resistance (R_{ic}). An extra pathway through a gap resistance (R_{gap}) representing partial cell coverage of the cell support, is included in the figure indicated by the dashed line and will be discussed in more detail in the next sections. Typically, the paracellular pathway is more dominant in the overall TEER, especially at the beginning of the barrier culture when adherent junctions or tight junctions between the cells have not yet formed. Please note that this model is only valid for the transfer of direct current (DC) signals. DC in this paper is defined as measurements using a constant current or potential, *i.e.* a signal of 0 Hz. However, this simplified model still applies for low-frequency alternating-current (AC) measurements, such as is used by some TEER measurement equipment described below.

In this framework, the total TEER is the equivalent resistance of R_{trc} and R_{pc} in parallel:

$$T_{TEER} = R_{trc} // R_{pc} = \frac{(R_A + R_B)\cdot(R_{tj} + R_{ic})}{(R_A + R_B) + (R_{tj} + R_{ic})} \quad (1)$$

Commercial systems to measure TEER, such as the EVOM2 (World Precision Instruments, Inc.) or the similar Millicell ERS-2 (Millipore) unit use a near DC (12.5 Hz) current of 10 μA and a 4-point measurement method with either silver/silver chloride (Ag/AgCl) chopstick electrodes or special chambers with patterned Ag/AgCl electrodes, which facilitate measurements of TEER in Transwell culture inserts. A summary of average TEER values measured in Transwell devices for various cell types is shown in Fig. 2 (a more detailed overview of this literature is included in Table S1†).

There are various factors that influence TEER, including the physical support that is used for cell culture[62] and temperature,[63,64] as well as the material, quality and surface state of the electrodes. It is clear from the data in Table S1† and Fig. 2 that TEER values fluctuate significantly for various cell types. Moreover, even TEER values for the same cell type vary greatly in different studies. Generally, the values reported for co-cultures are higher than those for monocultures. Judging from these data, it is apparent that TEER measurements show large variance that raises the question whether it is a suitable method to quantitatively compare specific barrier tightness in a reproducible and standardized manner.

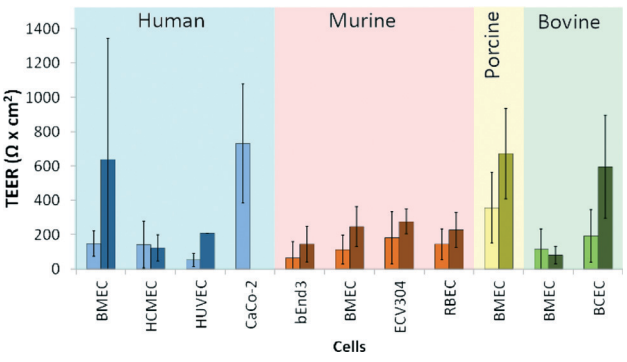

Fig. 2 TEER values for various cell types measured using a DC technique (Human,[3–26] Murine,[11,15–17,27–47] Porcine,[48–54] Bovine[55–61]). Light-colored bars indicate monocultures, while the darker-colored bars indicate co-cultures. For the exact cell types used in co-cultures and further details, see Table S1.†

In the literature, values for TEER in microfluidic chips are often different from those measured in Transwell systems using the same cell types.[65–69] Here, we show that these differences can result from specific measurement-related effects in microfluidic systems, rather than having a biological origin. TEER values measured in microfluidic devices also can vary greatly, and we demonstrate that this can be caused by small variations in cell confluency, which has a great impact on the measured TEER value. We focus on determining TEER by DC methods, as it is the main measurement method used in most past reports quantifying TEER values (Table S1†). In addition, we use the gut-on-a-chip[66,70] as a model organ-on-chip system to show how TEER measurements can differ when carried out in Transwell inserts *versus* microfluidic chips.

Theory

TEER in a microfluidic chip

To understand the theory behind TEER measurement in a microfluidic system, consider the simplified geometry of a typical organ-on-a-chip device, which consists of two parallel channels separated by a membrane with pores (Fig. 3a). In an equivalent circuit model of this fluidic chip (Fig. 3b), inlet and outlet channels l_a to l_d are depicted by resistors R_a to R_d. The parts of channels a–d and b–c that are connected by the membrane are indicated by l_{mem} (the length of the membrane) and the red dashed square. Therefore, the sum of resistors R_{T1} to R_{Tn-1} is equivalent to the reciprocal of the conductance of the top channel a–d over the length depicted by l_{mem}. Similarly, the sum of R_{B1} to R_{Bn-1} is equivalent to the resistance of the bottom channel b–c over length l_{mem}. Note that $R_{B1} = R_{B2} = R_{B3} = \ldots$ and so on, similarly for all resistances R_{Tx}. The actual value of each resistor R_{Tx} or R_{Bx} can be calculated using the following equation:

$$R_x = \frac{l_{mem}}{(n \cdot w_{ch} \cdot h_{ch} \cdot K)} \quad (2)$$

in which l_{mem} is the length of the channel above the membrane (in meter) and w_{ch} and h_{ch} the width and height of the channel (in meter), n the number of resistors included in the model (typically 1000 or more for accurate results), and K the conductivity (S m^{-1}) of the cell media inside the chip. The inlet and outlet resistors can be calculated using the same equation, by replacing l_{mem} with the length of the

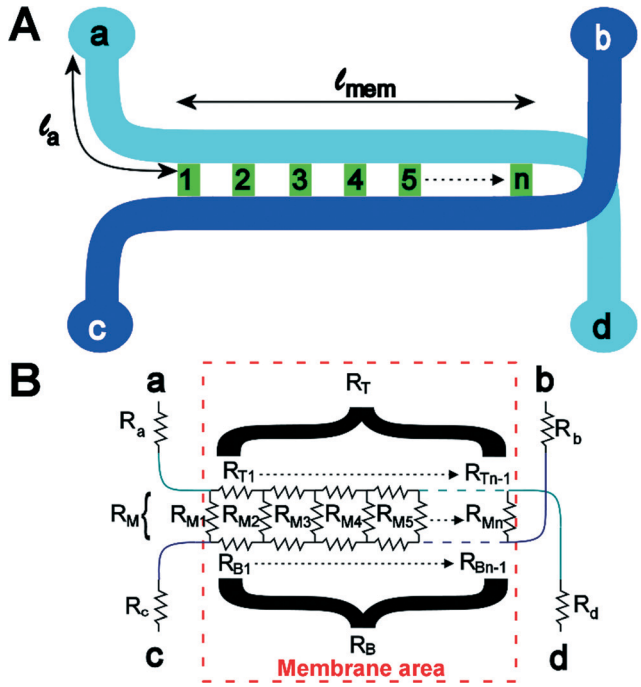

Fig. 3 Chip layout (A) and equivalent circuit (B) of the chip.

specific channel portion (*e.g.* l_a). For the membrane resistors R_{M1} to R_{Mn}, the value can be calculated by:

$$R_{Mx} = \frac{h_{mem}}{P \cdot w_{ch} \cdot \frac{l_{mem}}{n} \cdot K} + \frac{R_{TEER}}{\left(w_{ch} \cdot \frac{l_{mem}}{n}\right)} \quad (3)$$

with h^{mem} equal to the membrane thickness, P the porosity of the membrane (%) and R_{TEER} the TEER resistance (Ω m^2). The first term in eqn (3) describes the resistance due to the cell support (*e.g.* a polyester or polycarbonate membrane) and the second term, the resistance from the cell barrier. Please note that R_{TEER} would be the TEER measured in bulk systems, like Transwell inserts, where no significant potential differences can occur in the bulk of the liquid above and below the cell barrier.

The actual voltage drop and current distribution over the membrane can be calculated using two approaches. In the first approach, the equivalent model is approximated by a finite number of n resistors. Using Kirchhoff Matrix theory, the network can be solved, as explained in ESI.† The Kirchhoff Matrix approach is verified using an analytical model, which shows good agreement for TEER resistances above 50 Ω cm^2. However, the analytical model is difficult to solve for lower TEER values and does not allow the study of current distribution over the membrane. Therefore, only data generated with the Kirchhoff Matrix model are shown in this paper, but the analytical model is included in the ESI.†

It is possible to use the model to determine what would happen when one would do a DC measurement on the gut-on-a-chip to determine the TEER. Experimentally, one would first measure an empty device from a to b, thus determining the values of R_a, R_b, R_T, R_B and R_M together. Then, one would grow a layer of cells on the membrane, effectively increasing R_M. One would then measure the resistance of the device with cells and subtract the measurement from the empty device, and multiply the resulting value with the total membrane area. This yields the 'apparent TEER' of the cell layer in this device. It is this apparent TEER that is used in most papers reporting TEER in organ-on-a-chip systems. This apparent TEER can be calculated as:

$$R_{app,TEER} = (R_{(a-b),cells} - R_{(a-b),blank}) \cdot w_{ch} \cdot l_{mem} \quad (4)$$

Effect of cell monolayer coverage of the supporting substrate

The effect of cell monolayer coverage of the support membrane also can be studied using a model adapted from the circuit configuration shown in Fig. 1. The circuit was extended by adding a resistor describing a possible gap in the cell layer, parallel to the transcellular and paracellular pathways (dashed line and R_{gap} in Fig. 1). The resistance of this gap is equal to the membrane resistance only, as described by the first term of eqn (3), with n being equal to 1:

$$R_{gap} = \frac{h_{mem}}{(P \cdot w_{ch} \cdot l_{mem} \cdot K)} \quad (5)$$

Because R_{gap} is placed parallel with respect to the cell layer resistance R_{Mx} (with n = 1), it is possible to calculate the total resistance R_{tot} for Transwell systems as a function of cell coverage C varying between 0 (no coverage) and 1 (total cell confluence):

$$T_{tot} = \frac{(R_{Mx}(n=1)/C) \cdot (R_{gap}/(1-C))}{((R_{Mx}(n=1)/C) + (R_{gap}/(1-C)))} \quad (6)$$

Note that this equation is only valid for Transwell systems, since we use a system where R_{Mx} is simplified to a single resistor (n = 1). This is allowed as the potential is evenly distributed above and below the cell barrier in the Transwell culture device.

Experimental

Device geometry

To measure TEER under microfluidic conditions, on-chip measurements were performed using the gut-on-a-chip organ model.[66,70] The important geometric and electric parameters, which were also used for the model described in the previous section, are listed in Table 1.

Cell culture

Human intestinal epithelial Caco-2 BBE cells were obtained from the Harvard Digestive Disease Center, and routinely grown in Dulbecco's Modified Eagle Medium (DMEM; Gibco, Grand Island, NY, USA) containing 4.5 g L^{-1} glucose and 25 mM HEPES supplemented with 20% fetal bovine serum

Table 1 Parameters of the gut-on-a-chip organ model

Parameter	Value
w_{ch}	1000 μm
h_{ch}[a]	150 μm
l_{mem}	1 cm
l_a	5 mm
$R_a = R_b = R_c = R_d$	20 kΩ
$R_T = R_B$	39 kΩ
Cell line	Caco-2
Conductivity of culture medium	1.67 S m^{-1}

[a] The heights of the upper and lower microchannels are identical (150 μm).

(Gibco), 100 units mL^{-1} penicillin, and 100 μg mL^{-1} streptomycin (Gibco).

Cells were either seeded in Transwell inserts or in the gut-on-a-chip microfluidic devices, and maintained at 37 °C in a humidified incubator under 5% CO_2 in air.

For Transwell experiments, Caco-2 cells were seeded at a density of 1.5×10^5 cells cm^{-2} on porous, polyester, Transwell (Corning, Tewksbury, MA, USA) membrane inserts (0.33 cm^2, 0.4 μm pores) that were pre-coated with a mixture of type I collagen (rat tail, 50 μg mL^{-1}; Gibco) and Matrigel (300 μg mL^{-1}; BD Biosciences, Bedford, MA, USA) in serum-free DMEM for 2 hours. Culture medium was refreshed every other day on both the apical and basolateral side of a Transwell chamber.

For experiments in the gut-on-a-chip microdevices, the devices were prepared by flowing 70% (v/v) ethanol through the channels for sterilization, drying the entire system in a 60 °C oven overnight, and then immediately exposing them to ultraviolet light and ozone (UVO Cleaner 342, Jelight Company Inc., Irvine, CA, USA) for 40 min to activate the surface of microchannels. The gut-on-a-chip devices were then coated with the same mixture of collagen I and Matrigel as used in the Transwell cultures. Caco-2 cells were seeded into the upper microchannel at 1.5×10^5 cells cm^{-2} and allowed to attach under static conditions. After 1 hour, culture medium was perfused through the upper channel at 30 μL h^{-1} (fluid shear stress, 0.02 dyne cm^{-2}) for one day. Subsequently, medium was flowed through both the upper and lower channels at the same rate, and vacuum-driven stretching motions (10% in cell strain, 0.15 Hz in frequency) were applied through hollow side chambers to induce mechanical deformations on the cells using a pneumatic controller (FX5K Tension; Flexcell International Corporation, Hillsborough, NC).

TEER measurements

In Transwell cultures, TEER values were measured with a Millicell ERS meter (Millipore, Bedford, MA) and chopstick-like electrodes. TEER values were determined by subtracting the baseline resistance value of empty coated inserts. The TEER of a Caco-2 monolayer in the gut-on-a-chip microdevice was measured using a voltage-ohm multimeter (87V Industrial Multimeter, Fluke Corporation, Everett, WA, USA) coupled to Ag/AgCl electrodes (0.008" in diameter; A-M Systems, Inc., Sequim, WA, USA). The electrodes were inserted in the tubing of the inlet of the top channel of the microdevice (a in Fig. 3) and the outlet of the bottom channel of the microdevice (b). Again, the baseline resistance value measured in the absence of cells was subtracted from values of devices with a cell monolayer.

Results and discussion

TEER model

The theoretical model of the gut-on-a-chip device can be used to calculate what the apparent TEER of a measurement would be when cell layers with different TEERs would be growing in the device. Fig. 4 shows the apparent TEER of the gut-on-a-chip calculated from the Kirchhoff model, compared to the actual TEER value used in the model (R_{TEER} or Transwell TEER in eqn (3)). The apparent gut-on-a-chip TEER value is calculated from the potential drop between ports a–b, and an arbitrary current of 1A, which is applied between ports a–b, multiplied by the entire membrane area. Interestingly, the apparent TEER value calculated for the gut-on-a-chip is higher than the actual R_{TEER} (Transwell TEER) used in the model. For example, the apparent TEER value for a measurement in the gut-on-a-chip geometry would be 1550 Ω cm^2 if the actual (Transwell) TEER were 1000 Ω cm^2, given the same monolayer cell coverage. The differences are even more dominant for the lower range of actual (Transwell) TEER values. It is worth noting that the effect would be even more pronounced in microdevices with longer channels or smaller channel heights.

The reason for this theoretical deviation between apparent TEER and actual TEER in a microdevice with a gut-on-a-chip geometry becomes clear when studying the local current distribution in the device. Fig. 5 shows the normalized current distribution for the gut-on-a-chip geometry for low (1 Ω cm^2) and high (1001 Ω cm^2) TEER values through the membrane

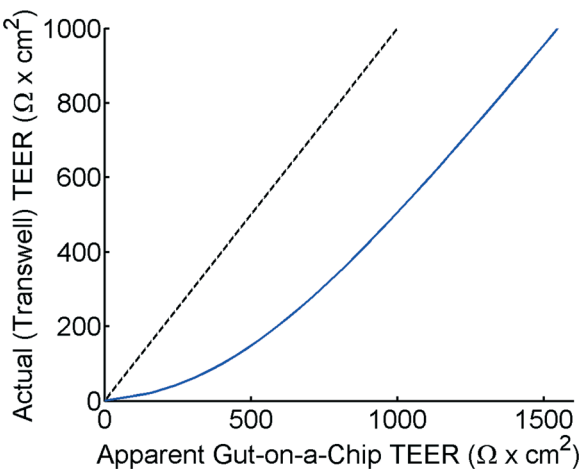

Fig. 4 Apparent TEER in a theoretical measurement on a microdevice with the gut-on-a-chip geometry *versus* the actual (Transwell) TEER value as used in the model. The dashed line is a guide for the eye to emphasize the deviation, showing $x = y$.

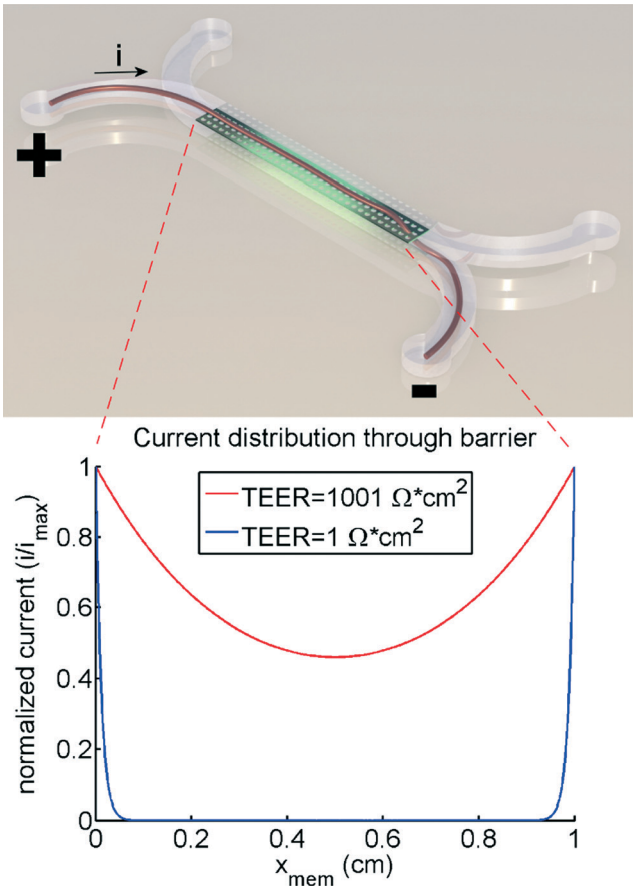

Fig. 5 Top, artist impression of the current (red line) flowing through the membrane, where the current density is depicted as a gradient from black to green (high to low). Bottom, calculated current distribution through the membrane over the length of the channel for low (1 Ω cm^2) and high (1001 Ω cm^2) TEER values using the geometry for the gut-on-a-chip.

area. At low TEER, any potential difference between top and bottom channel is almost immediately equalized at the beginning and end of the channel. With increasing TEER, more current flows through the entire membrane although still most current flows through the beginning and end part of the membrane.

Properly conducted Transwell TEER measurements are usually optimized by ensuring an equal current density through the entire membrane. In any case, conductivity of the culture medium is such that the bulk liquid in Transwell systems ensures an almost equal potential drop over the entire membrane. In microfluidic chips, this is clearly not always the case, as illustrated by Fig. 5. This is because conductance in the microfluidic channels is easily many orders of magnitude lower compared to the bulk. As a result, only part of the membrane is conducting current, therefore the apparent TEER in these chip systems will be higher than in a Transwell system with the same membrane area.

One of the ways to overcome this issue would be to integrate electrodes inside the top and bottom channel to ensure an equal potential drop over the entire membrane. Major drawbacks of that approach are that the electrodes will block the field of view and device fabrication will be more complicated and costly. Moreover, the electrodes are not immediately compatible with systems such as the gut-on-a-chip and lung-on-a-chip devices,[65] where mechanical deformations such as stretching are required.

Alternatively, the theoretical model described in this article can be used to convert the apparent TEER that is measured in a microfluidic chip to a TEER that can be compared with Transwell data using a calculated conversion graph, as shown in Fig. 6. Please note that this graph is calculated for the specific geometry of the gut-on-a-chip, but similar conversion graphs can easily be calculated for other geometries.

TEER measurements in Transwell *versus* gut-on-a-chip

Analysis of the same human intestinal epithelial Caco-2 cells grown in both the gut-on-a-chip and Transwell inserts revealed that the absolute TEER values measured in the gut-on-a-chip are consistently higher than those measured in the Transwell cultures (Fig. 6). The TEER measurements initially follow a similar trend in both systems; however, after approximately 70 hours TEER values in the gut-on-a-chip measurements keep increasing and become significantly higher than the TEER values measured in Transwell. This is likely because Caco-2 cells spontaneously undergo 3D villus morphogenesis from a 2D monolayer (Fig. S4b†) when the cells experience flow and peristalsis-like motions in the gut-on-a-chip, beginning about 3 days of culture.[66,70] The gut-on-a-chip displays intestinal villi and crypt characteristics with physiological growth up to several hundreds of microns in height, and increased expression of intestine-specific functions, including mucus production. In contrast, Caco-2 cells maintain a polarized, but flat monolayer under conventional static culture conditions (Fig. S4a†), which is observed even up to 2 months of culture. Thus, the increased TEER profile

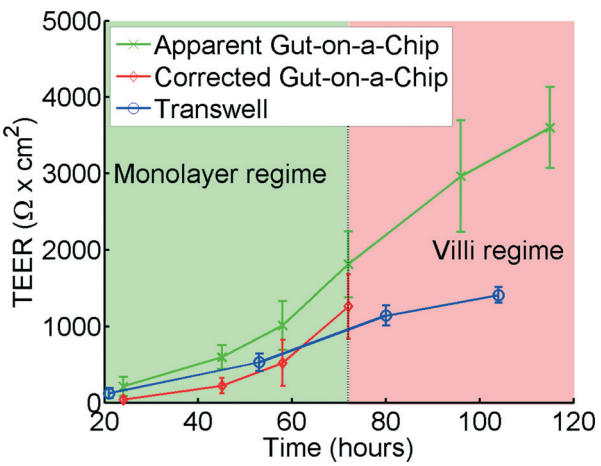

Fig. 6 TEER measurements for the gut-on-a-chip (green, x) and Transwell (blue, o) using human intestinal epithelial Caco-2 cells. The corrected gut-on-a-chip line (red, ◊), is calculated using the translational graph shown in Fig. 4, which is only valid in the monolayer regime. Error bars denote standard deviation. For chip measurements, n = 7, for Transwell measurements, n = 12.

after 72 hours may be attributed to enhanced intestinal differentiation, but the altered morphological features make it difficult to interpret using the present model.

Model and experimental agreement

Up to 60 hours, the model seems to predict the differences between the microfluidic chip and the Transwell quite accurately. Microscope observations confirm that after 72 hours the cells cultured in the gut-on-a-chip transform from a planar cell monolayer (Fig. S4b†) into three-dimensional villi-like structures (Fig. S4c†). Because the height of the villi reaches ~120 μm, the accessible space in the upper microchannel above the villi progressively decreases, which proportionally increases the resistance R_T in the top channel. This would account for the progressive increase in measured resistance at later time points in the gut-on-a-chip. The current model does not take this effect into account which would explain the differences between the model and the experimental results at times beyond 72 hours.

Effects of poor cell coverage when measuring TEER

In principle, the TEER parameter describes the quality of the barrier function of a cell layer. In our model, as shown in Fig. 1 and eqn (6), we discriminate between a paracellular pathway in the intact cell monolayer and a pathway through a gap in the monolayer. Fig. 7 shows the impact of a small gap in the monolayer due to partial cell coverage. As can be seen from this figure, even a minor defect in monolayer confluency will have a major impact on the measured TEER. For example, at 99.6% cell coverage the measured TEER value will be 80% lower than the TEER of a culture with full cell coverage. We believe that this is a major reason for the large variations observed in TEER measurements in literature. Even monolayers that show the expression of tight junctional proteins using fluorescent staining can have low TEER if small gaps are present (*e.g.* at the edge of the Transwell-insert or the microfluidic chip). The effects of cell coverage are of particular importance in microfluidic systems because of the relatively small surface area as well as the decreased effective surface area due to the unequal current distribution effect described in the previous sections.

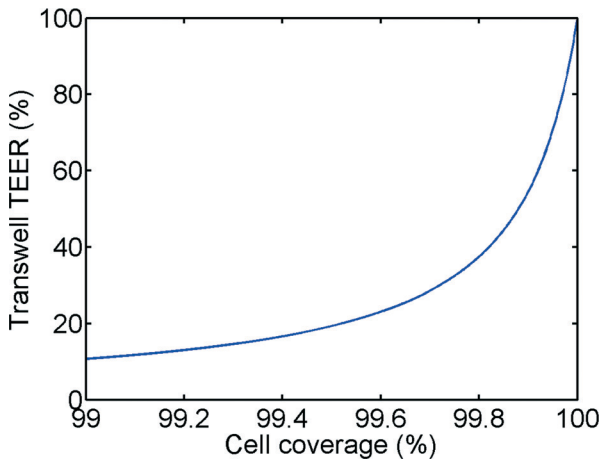

Fig. 7 Calculated relative Transwell TEER *vs.* cell coverage.

DC *versus* AC TEER measurements

In this and earlier papers, TEER in the gut-on-a-chip device is measured using a multimeter.[65,66] Special care needs to be taken if a multimeter is used to determine the resistance, as the applied voltage to the electrodes can vary significantly among manufacturers, models and also between various resistance measurement ranges. The used voltage can therefore influence the determination of TEER or in worst case depletes the Ag/AgCl electrode quickly leading to measurement errors and cell toxicity due to the release of silver ions.[71] Moreover, the Millicell ERS meter used for Transwell TEER measurements is not suited for the gut-on-a-chip device. The Millicell device uses a fixed current of 10 μA, which results in potentials that exceed the maximum measurable membrane potential of 200 mV due to the high resistance of the microchannels. For reproducibility, each TEER measurement in the gut-on-a-chip device was carried out with freshly prepared pair of Ag/AgCl electrodes as prolonged use of a single electrode would lead to undesired changes in resistance due to changes in the electrode surface. In both cases the TEER measurement is very sensitive to temperature variations.

Given the downsides of DC-based systems, complex-impedance based systems[72] have been developed for measuring TEER as well. The company Flocel Inc. is offering an AC measurement system, but it is tailored towards special proprietary cartridges used for cell culture and is therefore not easily transferable to organs-on-chips or Transwell systems. To our knowledge, the only AC systems commercially available to determine TEER in Transwell are the cellZscope system[72] (nanoAnalytics GmbH) and the ECIS system (Applied Biophysics).

In principle, the model presented here can be extended to include the cell membrane capacitance and the double layer capacitance at the electrode surface. Ultimately we expect that measurements using AC will allow direct determination of TEER by comparing the impedance at two distinctively different frequencies. Moreover, Ag/AgCl electrodes would be no longer required as measuring with AC enables the use of other (inert) electrode materials like platinum.

Conclusions

TEER measurements show large variations in literature, not only between various cell lines but also between different studies with the same cell lines. It also has been difficult to compare results obtained with different culture systems, such as Transwell culture inserts *versus* microfluidic organs-on-chips. Our results show that when measuring TEER in organ-on-a-chip systems, the confined environment of microfluidic channels results in higher values compared to Transwell. Our analysis also revealed that this seemingly higher TEER has a geometrical origin, rather than a biological one. Importantly, TEER measurements obtained in microfluidic systems can be

compared to those obtained in Transwell systems using the theoretical model and comparison method we presented here.

The cell coverage over the supporting substrate is also an important factor. Only the slightest gap (0.4%) can reduce the measured TEER significantly (80%). Even if fluorescent staining indicates a good barrier with tight junctions, TEER values might be lower if a small gap is present somewhere in the cell monolayer. We suspect that small defects in cell coverage are the main cause for large variations in measurements reported in literature.

Acknowledgements

We would like to thank B. de Wagenaar for fruitful discussions and assistance with the artwork, and T. Hamkins-Indik for her technical assistance. This research was sponsored by the Wyss Institute for Biologically Inspired Engineering at Harvard University and the Defense Advanced Research Projects Agency under Cooperative Agreement Number W911NF-12-2-0036. The views and conclusions contained in this document are those of the authors and should not be interpreted as representing the official policies, either expressed or implied, of the Defense Advanced Research Projects Agency, or the U.S. Government.

Notes and references

1 A. D. van der Meer and A. van den Berg, *Integr. Biol.*, 2012, **4**, 461–470.
2 N. J. Abbott, L. Rönnbäck and E. Hansson, *Nat. Rev. Neurosci.*, 2006, **7**, 41–53.
3 S. Man, E. E. Ubogu, K. A. Williams, B. Tucky, M. K. Callahan and R. M. Ransohoff, *Clin. Dev. Immunol.*, 2008, **2008**, 384982.
4 D. Wong, K. Dorovini-Zis and S. R. Vincent, *Exp. Neurol.*, 2004, **190**, 446–455.
5 M.-N. Lin, D.-S. Shang, W. Sun, B. Li, X. Xu, W.-G. Fang, W.-D. Zhao, L. Cao and Y.-H. Chen, *Brain Res.*, 2013, **1513**, 1–8.
6 F. Shimizu, Y. Sano, K. Saito, M. A. Abe, T. Maeda, H. Haruki and T. Kanda, *Neurochem. Res.*, 2012, **37**, 401–409.
7 L. B. Thomsen, T. Linemann, K. M. Pondman, J. Lichota, K. S. Kim, R. J. Pieters, G. M. Visser and T. Moos, *ACS Chem. Neurosci.*, 2013, **4**(10), 1352–1360.
8 K. Mishiro, M. Ishiguro, Y. Suzuki, K. Tsuruma, M. Shimazawa and H. Hara, *Neuroscience*, 2012, **205**, 39–48.
9 S. C. Wassmer, V. Combes, F. J. Candal, I. Juhan-Vague and G. E. Grau, *Infect. Immun.*, 2006, **74**, 645–653.
10 E. S. Lippmann, S. M. Azarin, J. E. Kay, R. A. Nessler, H. K. Wilson, A. Al-Ahmad, S. P. Palecek and E. V Shusta, *Nat. Biotechnol.*, 2012, **30**, 783–791.
11 G. V. Chaitanya, W. E. Cromer, S. R. Wells, M. H. Jennings, P. O. Couraud, I. A. Romero, B. Weksler, A. Erdreich-Epstein, J. M. Mathis, A. Minagar and J. S. Alexander, *J. Neuroinflammation*, 2011, **8**, 162.
12 Y.-C. Kuo and C.-H. Lu, *Colloids Surf., B*, 2011, **86**, 225–231.
13 K. Vu, B. Weksler, I. Romero, P.-O. Couraud and A. Gelli, *Eukaryotic Cell*, 2009, **8**, 1803–1807.
14 L. Cucullo, P.-O. Couraud, B. Weksler, I.-A. Romero, M. Hossain, E. Rapp and D. Janigro, *J. Cereb. Blood Flow Metab.*, 2008, **28**, 312–328.
15 N. Yamada, S. Nakagawa, S. Horai, K. Tanaka, M. A. Deli, H. Yatsuhashi and M. Niwa, *Microvasc. Res.*, 2014, **92**, 41–49.
16 Y. Xie, L. Ye, X. Zhang, W. Cui, J. Lou, T. Nagai and X. Hou, *J. Controlled Release*, 2005, **105**, 106–119.
17 S. M. Seok, J. M. Kim, T. Y. Park, E. J. Baik and S. H. Lee, *Arch. Pharmacal Res.*, 2013, **36**, 1149–1159.
18 G. Borchard, L. Luegen and A. G. De Boer, *J. Controlled Release*, 1996, **39**, 131–138.
19 M. El-sayed, M. Ginski and C. Rhodes, *J. Controlled Release*, 2002, **81**, 355–365.
20 B. J. De Leeuw, A. F. Kotze, J. C. Verhoef and H. E. Junginger, *J. Controlled Release*, 1998, **51**, 35–46.
21 A. F. Kotze, M. M. Hanou, H. L. Lueben, A. G. de Boer, J. C. Verhoef and H. E. Junginger, *J. Pharm. Sci.*, 1999, **88**, 253–257.
22 W. Tsuzuki, *Lipids*, 2007, **42**, 613–619.
23 V. Gusti, K. M. Bennett and D. D. Lo, *Physiol. Rep.*, 2014, **2**, 1–13.
24 A. Rodriguez-Gaztelumendi, M. Alvehus, T. Andersson and S. O. P. Jacobsson, *Toxicol. Lett.*, 2011, **207**, 1–6.
25 J. Smith, E. Wood and M. Dornish, *Pharm. Res.*, 2004, **21**, 43–49.
26 R. Jevprasesphant, J. Penny, D. Attwood, N. B. Mckeown and A. D. Emanuele, *Pharm. Res.*, 2003, **20**, 1543–1550.
27 G. Li, M. J. Simon, L. M. Cancel, Z. D. Shi, X. Ji, J. M. Tarbell, B. Morrison and B. M. Fu, *Ann. Biomed. Eng.*, 2010, **38**, 2499–2511.
28 R. Booth and H. Kim, *Lab Chip*, 2012, **12**, 1784.
29 D. M. Wuest, A. M. Wing and K. H. Lee, *J. Neurosci. Methods*, 2013, **212**, 211–221.
30 C. D. Hue, S. Cao, S. F. Haider, K. V. Vo, G. B. Effgen, E. Vogel, M. B. Panzer, C. R. D. Bass, D. F. Meaney and B. Morrison, *J. Neurotrauma*, 2013, **30**, 1652–1663.
31 A. Inamura, Y. Adachi, T. Inoue, Y. He, N. Tokuda, T. Nawata, S. Shirao, S. Nomura, M. Fujii, E. Ikeda, Y. Owada and M. Suzuki, *Neurochem. Res.*, 2013, **38**, 1641–1647.
32 M. A. Fleegal-DeMotta, S. Doghu and W. A. Banks, *J. Cereb. Blood Flow Metab.*, 2009, **29**, 640–647.
33 A. R. Calabria, C. Weidenfeller, A. R. Jones, H. E. De Vries and E. V. Shusta, *J. Neurochem.*, 2006, **97**, 922–933.
34 P. Demeuse, A. Kerkhofs, B. Knoops and C. Remacle, *J. Neurosci. Methods*, 2002, **121**, 21–31.
35 C. Weidenfeller, C. N. Svendsen and E. V. Shusta, *J. Neurochem.*, 2007, **101**, 555–565.
36 G. Shayan, Y. S. Choi, E. V. Shusta, M. L. Shuler and K. H. Lee, *Eur. J. Pharm. Sci.*, 2011, **42**, 148–155.
37 M. Honda, S. Nakagawa, K. Hayashi, N. Kitagawa, K. Tsutsumi, I. Nagata and M. Niwa, *Cell. Mol. Neurobiol.*, 2006, **26**, 109–118.

38 X. Jiang, M. Guo, J. Su, B. Lu, D. Ma, R. Zhang, L. Yang, Q. Wang, Y. Ma and Y. Fan, *Int. J. Alzheimer's Dis.*, 2012, **2012**, 109324.
39 J. X. Zhou, G. R. Ding, J. Zhang, Y. C. Zhou, Y. J. Zhang and G. Z. Guo, *Biomed. Environ. Sci.*, 2013, **26**, 128–137.
40 H. Zhu, Z. Wang, Y. Xing, Y. Gao, T. Ma, L. Lou, J. Lou, Y. Gao, S. Wang and Y. Wang, *J. Ethnopharmacol.*, 2012, **141**, 714–720.
41 A. S. Easton and N. J. Abbott, *Brain Res.*, 2002, **953**, 157–169.
42 K. Hayashi, S. Nakao, R. Nakaoke, S. Nakagawa, N. Kitagawa and M. Niwa, *Regul. Pept.*, 2004, **123**, 77–83.
43 S. Nakagawa, M. A. Deli, H. Kawaguchi, T. Shimizudani, T. Shimono, A. Kittel, K. Tanaka and M. Niwa, *Neurochem. Int.*, 2009, **54**, 253–263.
44 K. Toyoda, K. Tanaka, S. Nakagawa, D. H. D. Thuy, K. Ujifuku, K. Kamada, K. Hayashi, T. Matsuo, I. Nagata and M. Niwa, *Cell. Mol. Neurobiol.*, 2013, **33**, 489–501.
45 H. E. De Vries, M. C. M. Blom-Roosemalen, M. Van Oosten, A. G. De Boer, T. J. C. Van Berkel, D. D. Breimer and J. Kuiper, *J. Neuroimmunol.*, 1996, **64**, 37–43.
46 S. Dohgu, F. Takata, J. Matsumoto, M. Oda, E. Harada, T. Watanabe, T. Nishioku, H. Shuto, A. Yamauchi and Y. Kataoka, *Microvasc. Res.*, 2011, **81**, 103–107.
47 W. Neuhaus, M. Freidl, P. Szkokan, M. Berger, M. Wirth, J. Winkler, F. Gabor, C. Pifl and C. R. Noe, *Brain Res.*, 2011, **1394**, 49–61.
48 M. Smith, Y. Omidi and M. Gumbleton, *J. Drug Targeting*, 2007, **15**, 253–268.
49 C. R. W. Kuhlmann, C. M. Zehendner, M. Gerigk, D. Closhen, B. Bender, P. Friedl and H. J. Luhmann, *Neurosci. Lett.*, 2009, **449**, 168–172.
50 H. Franke, H. Galla and C. T. Beuckmann, *Brain Res. Protoc.*, 2000, **5**, 248–256.
51 H. Franke, H. J. Galla and C. T. Beuckmann, *Brain Res.*, 1999, **818**, 65–71.
52 A. Patabendige, R. A. Skinner, L. Morgan and N. Joan Abbott, *Brain Res.*, 2013, **1521**, 16–30.
53 W. Neuhaus, V. E. Plattner, M. Wirth, B. Germann, B. Lachmann, F. Gabor and C. R. Noe, *J. Pharm. Sci.*, 2008, **97**, 5158–5175.
54 Y. Zhang, C. S. W. Li, Y. Ye, K. Johnson, J. Poe, S. Johnson, W. Bobrowski, R. Garrido and C. Madhu, *Drug Metab. Dispos.*, 2006, **34**, 1935–1943.
55 O. C. Colgan, N. T. Collins, G. Ferguson, R. P. Murphy, Y. A. Birney, P. A. Cahill and P. M. Cummins, *Brain Res.*, 2008, **1193**, 84–92.
56 L. L. Rubin, D. E. Hall, S. Porter, K. Barbu, C. Cannon, H. C. Horner, M. Janatpour, C. W. Liaw, K. Manning and J. Morales, *J. Cell Biol.*, 1991, **115**, 1725–1735.
57 J. Haorah, D. Heilman, B. Knipe, J. Chrastil, J. Leibhart, A. Ghorpade, D. W. Miller and Y. Persidsky, *Alcohol.: Clin. Exp. Res.*, 2005, **29**, 999–1009.
58 P. J. Gaillard, L. H. Voorwinden, J. L. Nielsen, A. Ivanov, R. Atsumi, H. Engman, C. Ringbom, A. G. de Boer and D. D. Breimer, *Eur. J. Pharm. Sci.*, 2001, **12**, 215–222.
59 M. Salmeri, C. Motta, C. D. Anfuso, A. Amodeo, M. Scalia, M. A. Toscano, M. Alberghina and G. Lupo, *Cell. Microbiol.*, 2013, **15**, 1367–1384.
60 M. Boveri, V. Berezowski, A. Price, S. Slupek, A. M. Lenfant, C. Benaud, T. Hartung, R. Cecchelli, P. Prieto and M. P. Dehouck, *Glia*, 2005, **51**, 187–198.
61 M. P. Dehouck, S. Meresse, P. Delorme, J. C. Fruchart and R. Cecchelli, *J. Neurochem.*, 1990, **54**, 1798–1801.
62 C. M. Lo, C. R. Keese and I. Giaever, *Exp. Cell Res.*, 1999, **250**, 576–580.
63 T. S. Light, *Anal. Chem.*, 1984, **56**, 1138–1142.
64 L. Blume, M. Denker, F. Gieseler and T. Kunze, *Pharmazie*, 2010, **1**, 19–24.
65 D. Huh, B. D. Matthews, A. Mammoto, M. Montoya-Zavala, H. Y. Hsin and D. E. Ingber, *Science*, 2010, **328**, 1662–1668.
66 H. J. Kim, D. Huh, G. Hamilton and D. E. Ingber, *Lab Chip*, 2012, **12**, 2165–2174.
67 L. M. Griep, F. Wolbers, B. De Wagenaar, P. M. Braak, B. B. Weksler, I. A. Romero, P. O. Couraud, I. Vermes, A. D. Van Der Meer and A. Van Den Berg, *Biomed. Microdevices*, 2013, **15**, 145–150.
68 N. J. Douville, Y.-C. Tung, R. Li, J. D. Wang, M. E. H. El-Sayed and S. Takayama, *Anal. Chem.*, 2010, **82**, 2505–2511.
69 N. Ferrell, R. R. Desai, A. J. Fleischman, S. Roy, H. D. Humes and W. H. Fissell, *Biotechnol. Bioeng.*, 2010, **107**, 707–716.
70 H. J. Kim and D. E. Ingber, *Integr. Biol.*, 2013, **5**, 1130–1140.
71 C. Greulich, D. Braun, A. Peetsch, J. Diendorf, B. Siebers, M. Epple and M. Köller, *RSC Adv.*, 2012, **2**, 6981.
72 K. Benson, S. Cramer and H.-J. Galla, *Fluids Barriers CNS*, 2013, **10**, 5.

